CHAPTER 3
CONTINUOUS REACTOR DESIGN

To obtain the suitable method for producing biodiesel from high free fatty MCPO, transesterification was the fist method offered to observe the characteristic of reaction. It was found that FFA in MCPO is reacting with metallic alkoxide to produce soap (saponification). Then obtained soap induces other compositions in oil to convert into soap that caused low or without yield of methyl ester (ME). Therefore, it is necessary to reduce FFA in oil before starting the process for producing biodiesel. Although many methods could be solved the problem as above-mentioned, the two-stage was selected for producing biodiesel from this oil. Actually, the two-stage process consists of two methods: saponification followed by transesterification, and esterification followed by transesterification. Nevertheless, the latter two-stage process (esterification followed by transesterification) is offered in this investigation to produce biodiesel from oil containing high FFA in un-degummed state, because of short time and low production loss. In this procedure, acid catalyst esterification (the first stage) was employed to reduce FFA by converting it into biodiesel. Then, alkali catalyst transesterification was subsequently used to convert glycerides (triglyceride (TG), diglyceride (DG) and monoglyceride (MG)) into biodiesel.

Biodiesel has been traditionally produced using batch reactor technology. However, for obtaining a large amount of product in batch process, large size reactor, high energy consumption and high labor cost were required. In addition, the quality of the product in each batch was difficult to control. In order to reduce the batch process problem; therefore, the continuous process was investigated. Owing to requirement of low investment cost, suitability for liquid-liquid reaction and simply design in this investigation, a CSTR was selected for producing biodiesel from high free fatty acid MCPO via the two-stage process.

In design, the reaction rate of the two-stage process (batch reactor) in the previous work and the principle of chemical reactor design (unit operation and chemical kinetics) were necessary for the two-stage process continuous reactor.

3.1 n Tank Reactor in Series

Although continuous reactor can be classified into 3 types: continuous stirred tank reactors (CSTRs), plug flow reactor (PFR) and packed bed reactor (PBR), CSTRs are offered to produce biodiesel from high free fatty acid MCPO via the two-stage process in this investigation because it is low investment cost, suitable for liquid-liquid reaction and easy to design.

From the literature reviews, the number of researchers showed the amount and size of tank, but they did not show the technique for estimating tanks of CSTR. For example Darnoko, *et al.* (2000) produced biodiesel from palm oil by using a 1 litre CSTR tank and a 2 litres CSTR tank was used to produce biodiesel from soybean oil in Noureddini's experiment (Noureddini, *et al.*, 1998).

However, few researchers tried to estimate the amount and size of tank. For example, Leevijit, *et al.* (2004) investigated the design of 10 L/hr continuous reactor for palm oil transesterification. After studying the kinetics of tranesterification, the estimation of the amount of tank was investigated. The least-squares regression technique and solver tool in Microsoft Excel 2000 program was used in calculation. In addition, the efficiency of n CSTR tank was investigated the conversion at a various resident times in PFR by computing with MALAB (commercial program). Study showed that 6 ideal CSTR tank in series (2.272 litres in total) was suitable to be used in biodiesel production. Prateepchaikul, *et al.* (2009) investigated the design of esterification continuous reactor. The first procedure of his work was to estimate the amount of tank with kinetics of esterification for reducing FFA in MCPO (Jansri, 2007 and Jansri, *et al.*, 2011) and with the principle of the n tank reactor in series estimation (Fogler, 2006). After that, the suitable tank was determined by using retention time. the results indicated that 4 CSTR tanks in series (2.5 litres in total and feeding MCPO flow rate at 10 L/hr) was suitable for reducing high FFA containing in MCPO to less than 1 % wt/wt (0.035 mol/L).

Although, there were the number of researchers proposed the technique to design continuous reactor for reducing FFA and for producing biodiesel, this investigation

would like to thoroughly present other technique for estimating the amount of CSTR tanks in series.

3.1.1 Rate Law

The general equation for reversible reaction as shown in Equation 3.1 is indicated the reaction between reactant A and reactant B to form product C and product D. The reversible specific reaction rate coefficients (k_a and k_{-a}) are defined with respect to reactant A

$$aA + bB \underset{k_{-a}}{\overset{k_a}{\rightleftharpoons}} cC + dD \tag{3.1}$$

The rate of forward reaction indicates the disappearance of the reactant A, which defines the forward rate coefficient (k_a) with respect to reactant A as followed

$$r_{A.forward} = -k_a [A]^a [B]^b \tag{3.2}$$

The rate of reverse reaction indicates the appearance of the reactant A and the reverse rate coefficient (k_{-a}), which is defined with respect to reactant A as followed

$$r_{A.reverse} = k_{-a} [C]^c [D]^d \tag{3.3}$$

A mole balance for a constant volume reactor shows that the net rate of the reversible reaction is the sum of the reaction rate of the forward and the reverse reaction of reactant A as show in Equation 3.6.

$$r_A = k_{-a} [C]^c [D]^d - k_a [A]^a [B]^b \tag{3.4}$$

$$r_A = \frac{d[A]}{dt} \tag{3.5}$$

$$\frac{d[A]}{dt} = k_{-a}[C]^c[D]^d - k_a[A]^a[B]^b \tag{3.6}$$

3.1.1.1 Esterification

Esterification is the reaction for producing ester by converting the organic acid with alcohol as shown in Equation 3.7. This reaction can be reversed when it is treated with acid or base in aqueous solution (hydrolysis reaction).

$$R'COOH + HOR'' \overset{\text{catalyst}}{\rightleftharpoons} R'COOR'' + H_2O \tag{3.7}$$

In the two-stage process, esterification is used for converting FFA in the oil to biodiesel thus enabling the subsequent conversion of the triglyceride to biodiesel by transesterification. The FFA containing in the oil is converted into ester by reacting it with alcohol in the presence of sulfuric acid as catalyst as shown in Equation 3.8. However, it should be noted that this reaction is reversible:

$$FFA + HOR' \underset{k_2}{\overset{k_1}{\rightleftharpoons}} RCOOR' + H_2O \tag{3.8}$$

As a consequence, the rate of appearance of free fatty acid (FFA) can be presented as Equation 3.9. The rate of appearance of water is similarly presented as Equation 3.10.

$$\frac{d[FFA]}{dt} = -k_1[FFA]^a[AL]^b + k_2[E]^c[WT]^d \tag{3.9}$$

$$\frac{d[WT]}{dt} = k_1[FFA]^a[AL]^b - k_2[E]^c[WT]^d \tag{3.10}$$

3.1.1.2 Transesterification

Transesterification is a chemical process in which an acyl group in an ester is exchanged with a hydroxyl group in an alcohol thus generating a new alcohol and a new ester. In the production of biodiesel, the various acyl groups in the esters of the tri-hydric alcohol, 1, 2, 3-propanetriol (glycerol), are replaced with the hydroxyl groups of an alcohol such as methanol (CH_3OH) or ethanol (C_2H_5OH). This reversible reaction is facilitated by a catalyst and produces a new ester (biodiesel) and the tri-hydric alcohol (glycerol) as shown in Equation 3.11. The most common acyl groups in MCPO are the palmityl and stearyl group derived, respectively, from palmitic and stearic acids. However similar derivatives of other fatty acids may also be present.

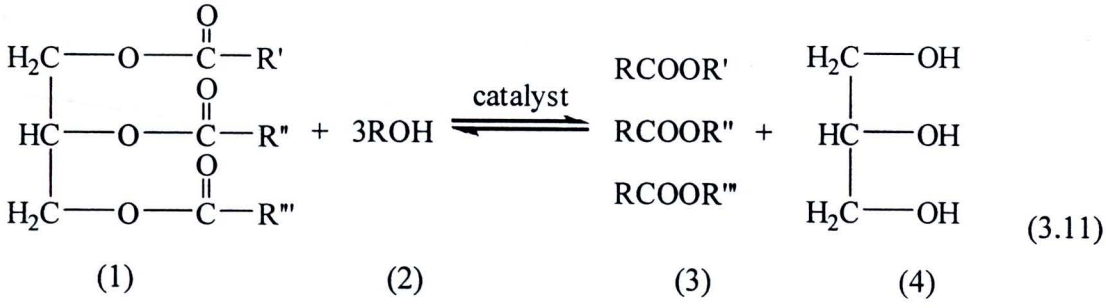

(3.11)

The overall transesterification reaction (Equation 3.11) takes place in three successive stages. The corresponding rate equations for the appearance of triglyceride (TG), diglyceride (DG), monoglyceride (MG), alcohol (AL), ester (E) and glycerol (GL) are given in Equation 3.12. All of reactions are reversible and are of pseudo-secondary order overall.

$$\frac{d[TG]}{dt} = -k_3[TG][AL] + k_4[DG][E]$$

$$\frac{d[DG]}{dt} = k_3[TG][AL] - k_4[DG][E] - k_5[DG][AL] + k_6[MG][E]$$

$$\frac{d[MG]}{dt} = k_5[DG][AL] - k_6[MG][E] - k_7[MG][AL] + k_8[GL][E]$$

$$\frac{d[GL]}{dt} = k_7[MG][AL] - k_8[GL][E]$$

$$\frac{d[E]}{dt} = k_3[TG][AL] - k_4[DG][E] + k_5[DG][AL] - k_6[MG][E] + k_7[MG][AL] - k_8[GL][E]$$

$$\frac{d[AL]}{dt} = -\frac{d[E]}{dt} \tag{3.12}$$

3.1.2 Rate Coefficients

Previous work, the biodiesel production from high FFA mixed crude palm oil (> 0.8 wt% of oil) by using the two-stage process (esterification followed by transesterification) was investigated in batch process based on parameters such as the speed of stirrer, the catalyst concentration, the amount of methanol, and reaction temperature. It was found that the suitable condition for reducing high FFA in MCPO (8-12 wt% oil) by using esterification was a 10:1 molar ratio of methanol to FFA and 10 wt% H_2SO_4 of FFA. As for ME production from the first solution by transesterification, it was found that the suitable condition was a 6:1 molar ratio of methanol of TG (triglyceride) in MCPO and 0.6 wt% sodium hydroxide of TG in MCPO. Both of reactions were carried out for 20 minutes under a 300 rpm speed of stirrer at 60°C. The samples were analyzed the concentration of TG, DG (diglyceride), MG (monoglyceride), FFA, and ME (methyl ester) by TLC/FID, the concentration of water by Karl Fischer, and the concentration of FFA, GL (glycerol) and NaOH (for neutralizing acid value in the first stage solution) by titration technique. The analyzed data were used to calculate the rate coefficients and the reaction orders of two-stage process by using curve-fitting tool of MATLAB as show the results in Equation 3.13-3.20.

$$r_{FFA} = -1.340C_{FFA}^{0.5}C_{AL}^{0.5} + 0.682C_E^{0.5}C_{WT}^{0.5} \tag{3.13}$$

$$r_{WT} = 1.340C_{FFA}^{0.5}C_{AL}^{0.5} - 0.682C_E^{0.5}C_{WT}^{0.5} \tag{3.14}$$

$$r_{TG} = -2.600C_{TG}C_{AL} + 0.248C_{DG}C_E \tag{3.15}$$

$$r_{DG} = 2.600C_{TG}C_{AL} - 0.248C_{DG}C_E - 1.186C_{DG}C_{AL} + 0.227C_{MG}C_E \tag{3.16}$$

$$r_{MG} = 1.186C_{DG}C_{AL} - 0.227C_{MG}C_E - 2.303C_{MG}C_{AL} + 0.022C_{GL}C_E \tag{3.17}$$

$$r_{GL} = 2.303C_{MG}C_{AL} - 0.022C_{GL}C_E \tag{3.18}$$

$$r_E = 2.600C_{TG}C_{AL} - 0.248C_{DG}C_E + 1.186C_{DG}C_{AL} - 0.227C_{MG}C_E + 2.303C_{MG}C_{AL} - 0.022C_{GL}C_E \quad (3.19)$$

$$r_{AL} = -r_E \quad (3.20)$$

3.1.3 The Rate Determining Step

Generally, the chemical reactions occur from the mechanism more than one elementary step, which is controlled by its rate coefficient and activation energy. Often one of the steps is slower than the others; therefore, the overall reaction rate can not exceed the rate of the slowest elementary step of its mechanism. So that the rate-determining step is controlled by the slowest step because it is the overall reaction limitation.

Table 3.1 The initial concentration of components in MCPO and de-acidified MCPO

Esterification			
Initial components	**Initial concentration** (mol/L)	**Product components**	**Product concentration** (mol/L)
FFA	0.359	FFA	0.018
AL	2.813	AL	2.541
ME	0.051	ME	0.322
WT	0.050	WT	0.255
Transesterification			
Initial components	**Initial concentration** (mol/L)	**Product components**	**Product concentration** (mol/L)
TG	0.806	TG	0.020
DG	0.096	DG	0.010
MG	0.016	MG	0.007
ME	0.269	ME	2.502
AL	6.119	AL	3.886
GL	0.000	GL	1.818

Equation 3.13-3.20 are used to determine the rate determining step of esterification and transesterification (feeding MCPO flow rate at 50 L/hr) using the initial concentration of main components in MCPO and de-acidified MCPO, respectively, which are analyzed by TLC/FID and titration technique as shown the values in Table 3.1.

It was found that Equation 3.13 was the rate determining step of esterification because it was the slowest elementary of its mechanism as shown the reaction rate in Table 3.2. Although reaction rate of alcohol disappearance was the slowest reaction rate in

transesterification as shown the reaction rate in Table 3.2, its rate law was not considered because the excess of alcohol was used as a main reagent in the reaction. Therefore, the rate law of TG disappearance (Equation 3.15) was used to determine the reaction step because it was the second slower reaction rate in transesterification.

Table 3.2 Reaction rate of esterification and transesterification

Rate of esterification	**Reaction rate** ($mol \cdot L^{-1} \cdot min^{-1}$)
r_{FFA}	-1.312
r_{WT}	0.091
Rate of transesterification	**Reaction rate** ($mol \cdot L^{-1} \cdot min^{-1}$)
r_{TG}	-12.816
r_{DG}	-0.501
r_{MG}	-0.183
r_{GL}	0.054
r_{E}	0.201
r_{AL}	-13.738

3.1.4 Rate Law of Esterification and Transesterification in Flow System

Fogler (2006) explained that, in the flow system, the concentration of reagent A determines from the molar flow rate and the volumetric flow rate of it as shown in Equation 3.21.

$$C_A = \frac{F_{A1}}{\nu} = \frac{\text{moles}}{\text{litre}} \tag{3.21}$$

The concentration of reagent A and B and Product C and D in Equation 3.1 can be written in term of their respective entering molar flow rates, the conversion and the volumetric flow rate as shown in Equation 3.22.

$$C_A = \frac{F_A}{\nu} = \frac{F_{A0}}{\nu}(1-X)$$

$$C_B = \frac{F_B}{\nu} = \frac{F_{B0} - (b/a)F_{A0}X}{\nu}$$

$$C_C = \frac{F_C}{\nu} = \frac{F_{C0} - (c/a)F_{A0}X}{\nu}$$

$$C_D = \frac{F_D}{\nu} = \frac{F_{D0} - (d/a)F_{A0}X}{\nu} \tag{3.22}$$

For the flow system of liquid phase concentrations, the volume change in each reaction is negligible. Consequently, the concentration of reagent B and product C and D can be determined on the initial concentration A and the conversion as shown in Equation 3.23. Finally, the equations of the liquid phase flow system give the rate law in term of conversion.

$$C_A = C_{A0}(1-X)$$

$$C_B = C_{B0} - (\frac{b}{a})C_{A0}X$$

$$C_C = C_{C0} - (\frac{c}{a})C_{A0}X$$

$$C_D = C_{D0} - (\frac{d}{a})C_{A0}X \qquad (3.23)$$

The rate determining step of esterification and transesterification in biodiesel production two-stage process (Equation 3.13-3.20) could be shown in the term of conversion by using the principle of the flow system of liquid phase concentrations (Equation 3.23) and the initial components concentration (Table 3.1) as shown in Equation 3.24 and 3.25, respectively.

$$-r_{FFA} = 0.223X - 1.585X^{0.5} + 1.274 \qquad (3.24)$$

$$-r_{TG} = 1.529X^2 - 14.451X + 13.961 \qquad (3.25)$$

3.1.5 Estimation of n Tanks Reactor in Series for Continuous Stirred Tank Reactors

Reactors in this investigation are connected in series in order that the exit stream of one reactor is the initial mixture of another reactor as shown in Figure 3.1. In a combination of CSTRs, X_1 at point i=1 is the achievement conversion in the first CSTR but X_2 at point i=2 is the total achievement conversion by all two reactors. Hence, to estimate the n tanks reactor, experimental data of batch system that give the reaction rate at difference conversions is used.

Conversion, reactor size or the amount of tanks of the first and second reactors as shown in Figure 3.1 can be calculated by combining a mole balance on each reactor and the molar flow rate at each point and rearranging as shown in Equation 3.26 and 3.27.

This principle of the continuous flow system in series is used to estimate the amount of tanks in series of esterification and transesterification of this study by calculating until it reaches the required conversion.

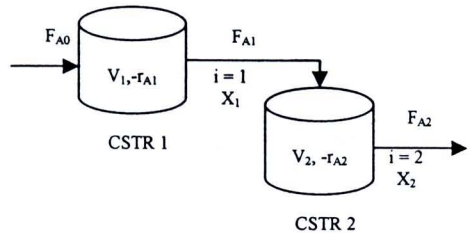

Figure 3.1 Two tanks reactor in series for continuous stirred tank reactors

Reactor 1: $$V_1 = F_{A0}\left(\frac{1}{-r_{A1}}\right)X_1 \qquad (3.26)$$

Reactor 2: $$V_2 = F_{A0}\left(\frac{1}{-r_{A2}}\right)(X_2 - X_1) \qquad (3.27)$$

3.1.5.1 Esterification

The esterification continuous process was required to reduce 8-12 wt% in MCPO to less than 1 wt%. That was the requirement conversion of FFA in MCPO was 0.92 (Jansri, 2007). To achieve the requirement, the volume of each tank was fixed at 0.5, 1.0 and 2.0 litre, rate law of esterification in flow system (Equation 3.24) and the principle of the continuous flow system in series were used to estimate the amount of tanks in series.

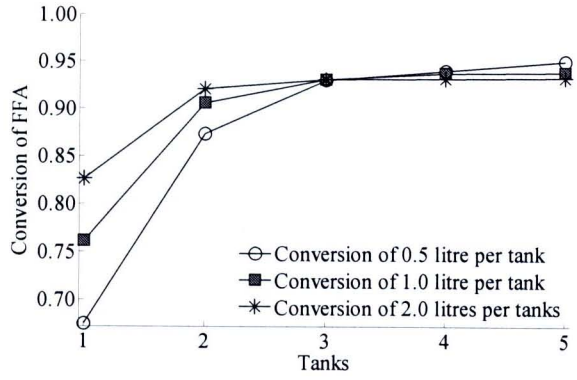

สำนักงานคณะกรรมการวิจัยแห่งชาติ ห้องสมุดงานวิจัย

Figure 3.2 The relation between the amount of tank and FFA conversion in esterification

The results in Figure 3.2 indicated that at the volume of 0.5 and 1.0 litre per tank, the requirement conversion (0.92) was reached for 3 tanks in series (1.5 and 3 liters of the total volume, respectively). In addition, 2 tanks in series could reach the conversion of esterification, when the 2.0 litre per tank (4 L in the total volume) was used to calculation.

3.1.5.2 Transesterification

The conversion at 0.99 was the requirement for converting TG, DG and MG in de-acidified MCPO into biodiesel (Jansri, 2007). Similar to the estimation of the number of tank of esterification, the predetermined fixed volume of each tank, the rate law of transesterification in flow system (Equation 3.25) and the principle of the continuous flow system in series were used. Figure 3.3 showed that the fixed volume at 1.0 litre per tank was satisfied the requirement of ME conversion by using 3 tanks of CSTR (3.0 L in total volume). In addition, when the fixed volume at 2.0 L per tank was used for calculation, 2 tanks of CSTRs (4.0 L in total volume) were reached the conversion. On the other hand, when the fixed volume at 0.5 litre per tank was used to calculation, the conversion was not reached the requirement.

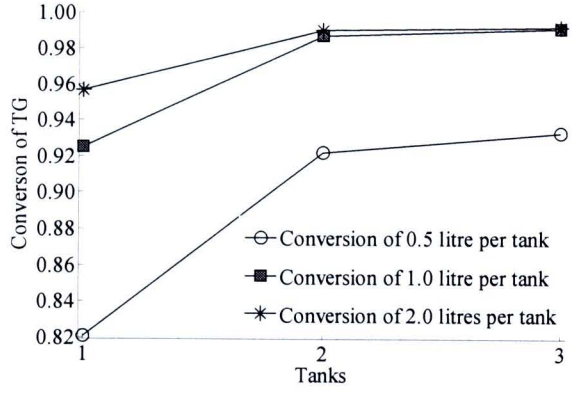

Figure 3.3 The relation between the amount of tank and ME conversion in transesterification

3.1.6 Retention Time for Determining the Amount and Volume of Tank in the Two-Stage Process Continuous Flow System

Although the number of tanks could be estimated by calculating with the rate law of the two-stage process and the principle of the continuous flow system in series, the definite number and volume of tank could not be determined. In addition, due to MeOH having high vapor pressure, the remaining MeOH in de-acidified MCPO (production of esterification) can evaporate continuously. Therefore, to minimize methanol evaporation, retention time for feeding solution to the second-stage process was adopted to determine the required capacity of reactor.

$$\tau = \frac{V}{\nu_0} \tag{3.28}$$

The results in Table 3.3 estimating retention time with Equation 3.28 indicated that the combination between esterification reactor total volume of 1.5 L separated into 3 tanks and 3 L reactor separated into 3 tanks of transesterification reactor could reach the requirement because of the small of theirs retention time lag.

Additionally, the required conversion of this process could also reach when 3 tanks (3.0 L of total volume) of both reactors were combined. However, it was found that the retention of transesterification reactor in Table 3.3 was smaller than esterification reactor. This caused, for a long time, esterification reactor could be not promptly supplied de-acidified MCPO to feed as a raw material in transesterification. Moreover, although the same conversion can be achieved with smaller size of tanks, larger size is required, hence, larger amount of reagents and longer retention time. Therefore, the first combination of reactor was selected to confirm in the next step.

Table 3.3 Retention time of each CSTR using in esterification and transesterification

Esterification

Tank	Total volume (L)	Conversion	Retention time (min)
1	2.00	0.827	2.14
2	4.00	0.921	4.27
3	6.00	0.931	6.41

Tank	Total volume (L)	Conversion	Retention time (min)
1	1.00	0.762	1.07
2	2.00	0.906	2.14
3	3.00	0.931	3.20

Tank	Total volume (L)	Conversion	Retention time (min)
1	0.50	0.675	0.53
2	1.00	0.874	1.07
3	1.50	0.930	1.60

Transesterification

Tank	Total volume (L)	Conversion	Retention time (min)
1	2.00	0.957	1.95
2	4.00	0.990	3.90
3	6.00	0.992	5.85

Tank	Total volume (L)	Conversion	Retention time (min)
1	1.00	0.925	0.98
2	2.00	0.987	1.95
3	3.00	0.991	2.93

Tank	Total volume (L)	Conversion	Retention time (min)
1	0.50	0.821	0.49
2	1.00	0.922	0.98
3	1.50	0.933	1.46

3.1.7 Verification of the Amount of CSTR Tank

Make certain that the adjudged number of tanks (Table 3.3) could be used for producing de-acidified MCPO and biodiesel. Therefore, the number of tanks for reducing FFA and for producing biodiesel from MCPO was confirmed under the selected reactor capacity by the Damköhler number and analyzing with the ASPEN PLUS Simulation Engine shown in Figure 3.4-3.7. Each reactor was separated into 1, 2 and 3 tanks, respectively, by fixing the total volume at 1.5 and 3 L for esterification and for transesterification, respectively. Then the tank number was verified by Damköhler number.

In numerical analysis, the initial conditions (Table 3.1), reaction temperature, the rate law, and the number and size of CSTR tank were installed in the program for verifying the number of CSTR tank. The results in each step were printed in term of mass flow rate and then they were converted into term of conversion. Obtained esterification and transesterification conversion from three different methods were then compare and the conversion that closely matched among the 3 methods was selected

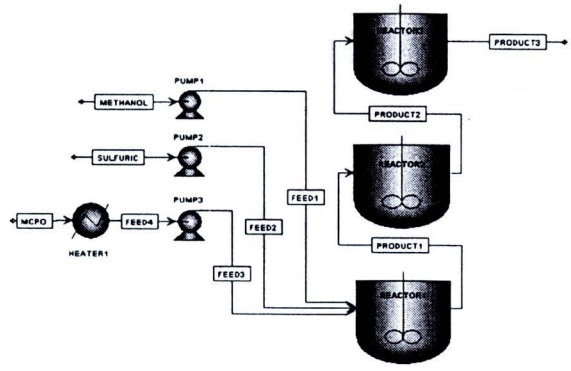

Figure 3.4 ASPEN PLUS Simulation Engine model for analysis the number of esterification CSTR tank

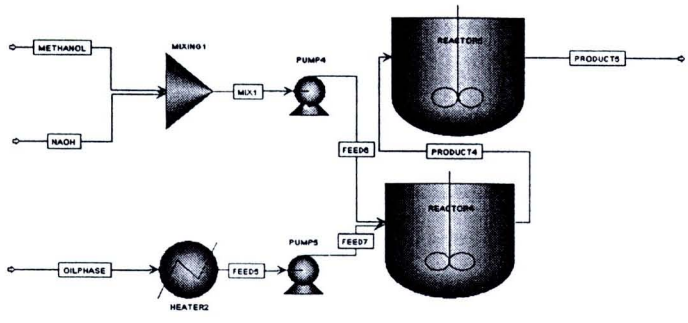

Figure 3.5 ASPEN PLUS Simulation Engine model for analysis the number of transesterification CSTR tank

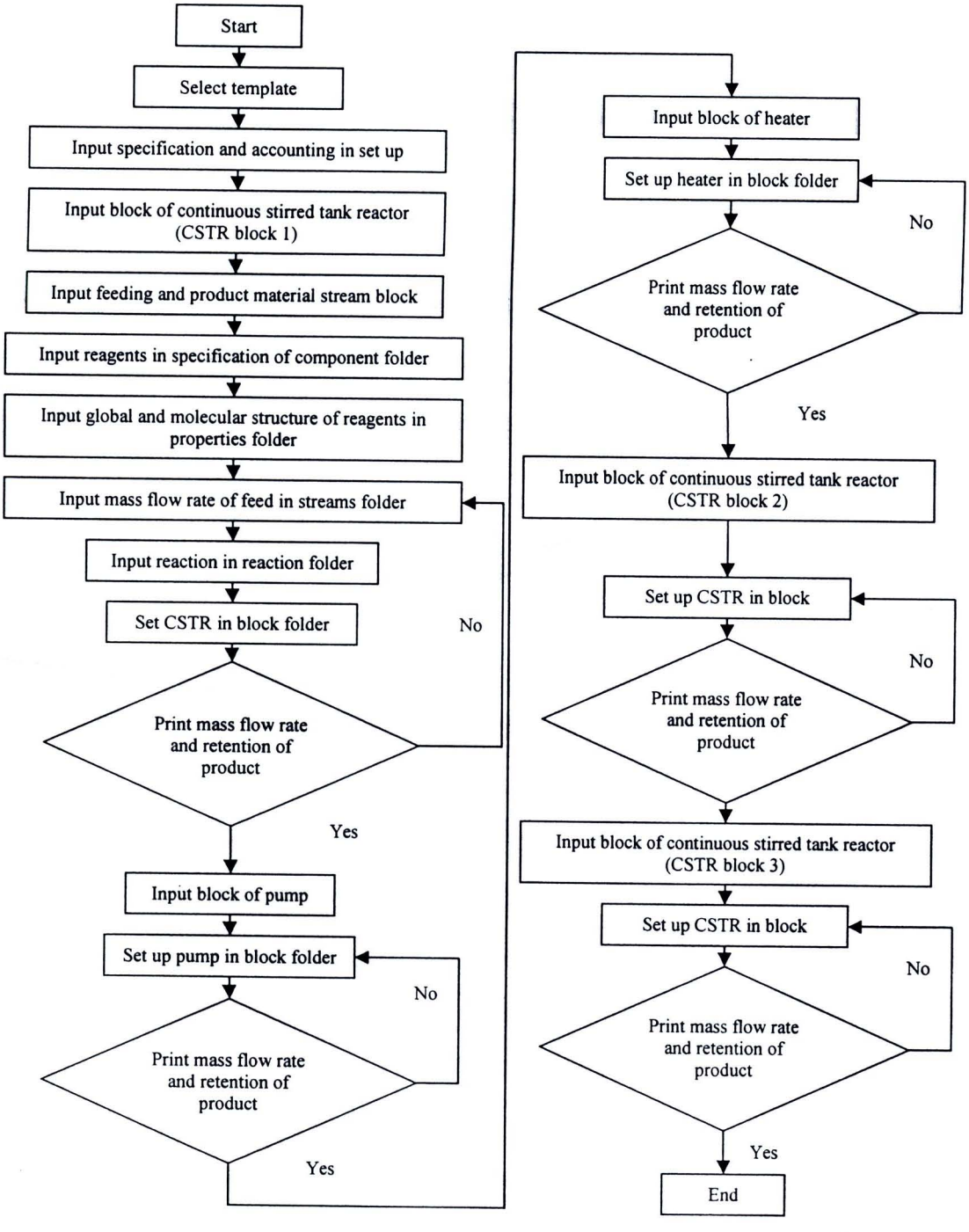

Figure 3.6 Diagram for analysis the number of esterification CSTR tank

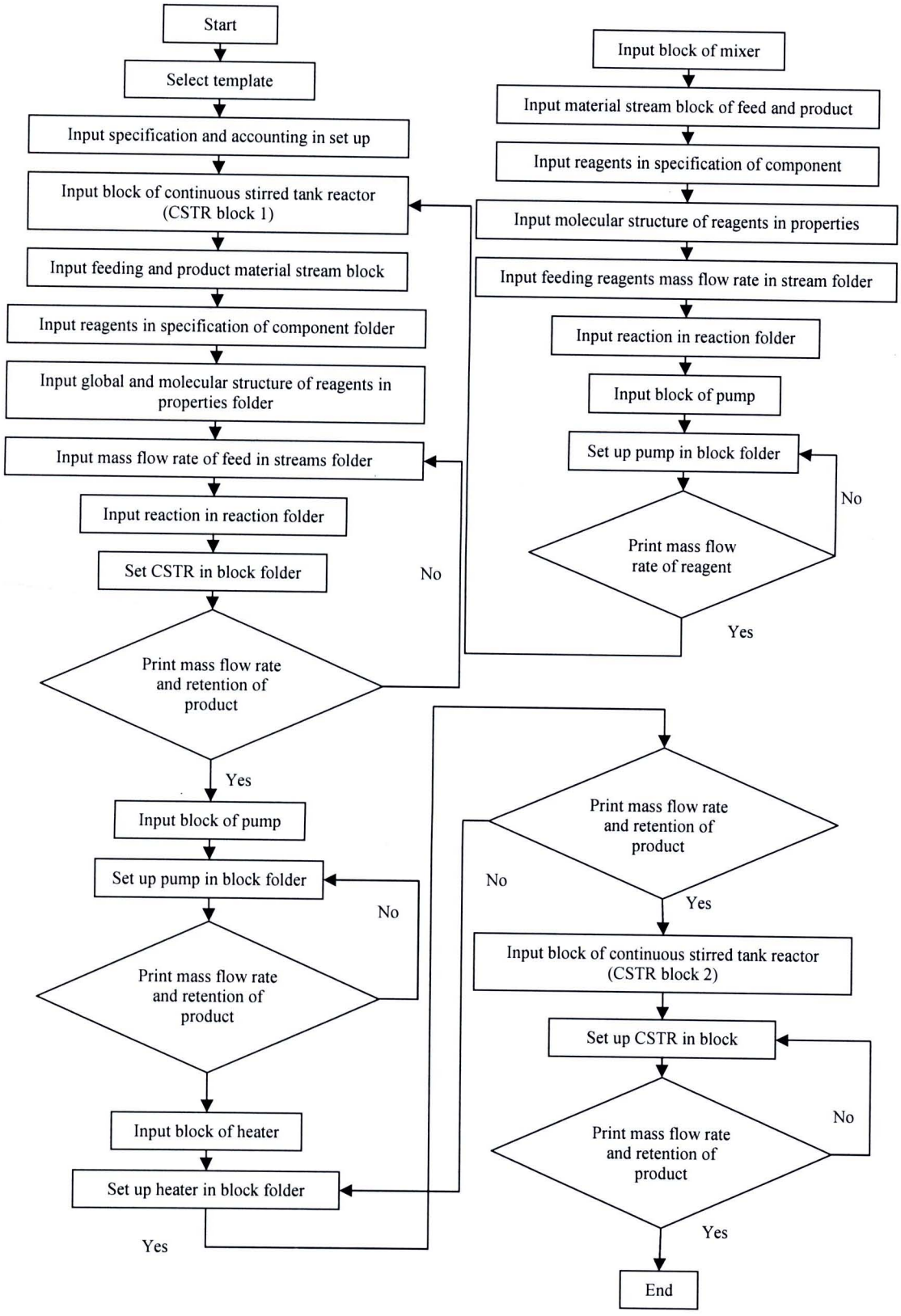

Figure 3.7 Diagram for analysis the number of transesterification CSTR tank

The perspective on the conversion and retention time of all estimation technique in each tank as shown in Table 3.4 was rather similar except for the retention time of FFA conversion. The reason for high error of reaction time for reducing FFA that was obtained from simulation was not exactly known. Likewise, the simulation data of transesterification in Table 3.4 showed that the conversion of ME could not reach the requirement of 99%. In presumption, both errors might have occurred in the boundary of retention time proceeding to steady state that set in this commercial program. However, this investigated focused on prediction about the number of tanks before fabrication. The results in Table 3.4 showed that 3 and 2 tanks were the most suitable number of tank for reducing FFA and producing biodiesel, respectively because they achieved the requirement for reaction conversion.

Table 3.4 Verification the suitable amount of tank by fixing the reactor volume

Total volume (L)	**Separated tanks**	**FFA conversion** (0.92)			**Retention time** (min)	
		Design	**Simulation**	**Damköhler number**	**Design**	**Simulation**
1.5	1	0.800	0.989 (23.62%)*	0.854 (6.75%)*	1.60	0.90 (43.75%)*
	2	0.895	0.990 (10.61%)*	0.979 (9.38%)*		
	3	0.930	0.990 (6.45%)*	0.997 (7.20%)*		
Total volume (L)	**Separated tanks**	**ME conversion** (0.99)			**Retention time** (min)	
		Design	**Simulation**	**Damköhler number**	**Design**	**Simulation**
3	1	0.968	0.904 (6.61%)*	0.979 (1.14%)*	2.93	2.68 (8.53%)*
	2	0.991	0.905 (8.68%)*	0.999 (0.81%)*		
	3	0.991	0.905 (8.68%)*	0.999 (0.81%)*		

*error

3.1.8 The Limited of FFA and TG Content in MCPO

Even though the simulation data indicated that 3 and 2 tanks CSTR could be reduced FFA and produced ME reached the requirement under the suitable batch condition, the reactor was not demonstrated its' performance. Therefore, the highest amount of FFA and of TG content that could be used in each reactor was investigated by simulation again.

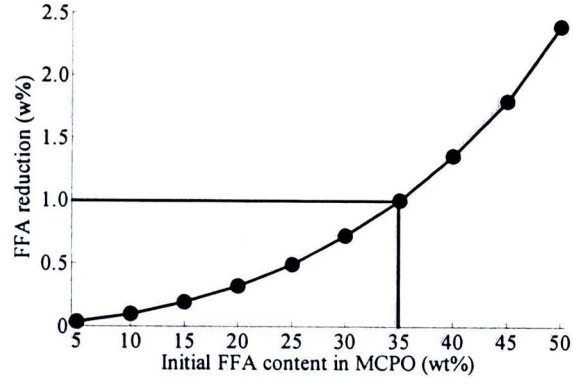

Figure 3.8 The limited concentration of initial FFA concentration using in esterification CSTR by simulation with ASPEN PLUS Simulation Engine

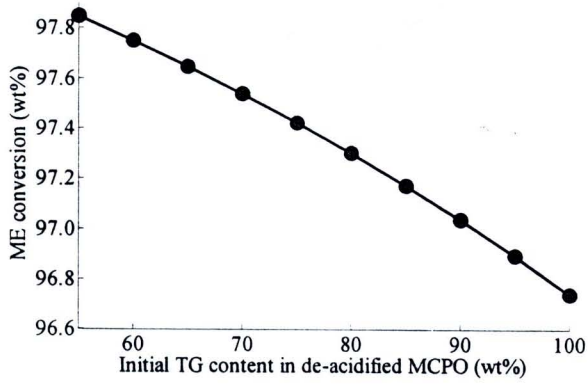

Figure 3.9 The limited concentration of initial TG concentration using in transesterification CSTR by simulation with ASPEN PLUS Simulation Engine

However, the concentration of FFA, TG, DG, MG, ME and WT were adjusted to a contrast between the mass fraction of MCPO composition (getting from the batch condition) and the assumption of an increase of FFA and TG content in MCPO. The results indicated that 35 wt% of FFA in MCPO (Figure 3.8) and 100 wt% of TG in de-acidified MCPO (Figure 3.9) were the highest concentration of FFA and TG could be used in the CSTR.

3.1.9 Conclusions

This investigation indicated that although larger size could be achieved the predetermined conversion, larger amount of reagents and longer time of reaction were required. Therefore, smaller size that matched retention time was selected to produce biodiesel via the two-stage process. The suitable tank number for reducing FFA in MCPO to less than 1 wt% (conversion more than 0.92) and for producing biodiesel from de-acidified MCPO to more than 97 wt% (conversion more than 0.99) were 3 tanks (1.5 L in total volume) and 2 tanks (3 L in total volume), respectively. Moreover, 35 wt% of FFA in MCPO and 100 wt% of TG in de-acidified MCPO were the highest FFA and TG concentration could be used in the CSTRs that were designed in this work.

3.2 Continuous Stirred Tank Reactors Agitations

This work focuses on changing of physical property oil and increasing the reaction rate of liquid-liquid mixing. Therefore, the agitations were designed for mixing immiscible reagent in esterification and in transesterification under ambient pressure at 60 °C will be investigation.

Before estimating the dimension of reactor agitations, three main composition of reactor agitation: tank, buffer and impeller were appreciated the physical properties of their type as followed.

3.2.1 Tank

Frequently, vertical cylindrical reactor having a cover is used as an agitated vessel for liquid-liquid mixing. The preferred bottom of the vessel is in 3 shapes such as round, flat and cone. Nevertheless, the reactor should not in cubic configuration because the reactor has shape corners and area, which fluid currents would not penetrate.

3.2.2 Baffle

Baffles are installed vertical strips perpendicular to the wall of the tank for controlling the fluid flow pattern. For the liquid having viscosity less than 20000 cP and for mixing in turbulence, baffles can be protected the circulatory and swirling flow pattern as shown in Figure 3.10.

However, the liquid in tank with installing baffles can not penetrate any tank area as show in Figure 3.11. Therefore, when baffles are installed in reactor, it should be spaced out reactor wall as shown in Figure 3.12.

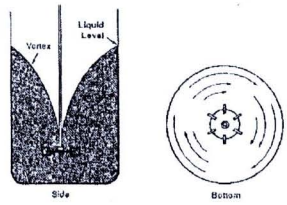

Figure 3.10 Swirling flow pattern with a radial-flow turbine in un-baffled reactor (McCabe, *et al.*, 2001)

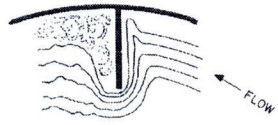

สำนักงานคณะกรรมการวิจัยแห่งชาติ ห้องสมุดงานวิจัย

Figure 3.11 Non-penetration area (Holland, *et al.*, 1966)

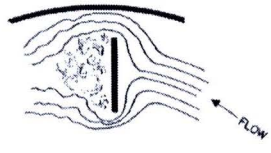

Figure 3.12 Leaving a space for protecting non-penetration area (Holland, *et al.*, 1966)

3.2.3 Impeller

Impeller is used to mix the heterogeneous liquids. Impeller can be categorized into 2 groups, which are axial-flow impellers (an axis of the impeller shaft) and radial-flow impellers (a radial and a tangential direction) as shown in Figure 3.13. In addition, the viscosity of liquids is indicated to determine the suitable impeller type for mixing the liquid as shown in Figure 3.14.

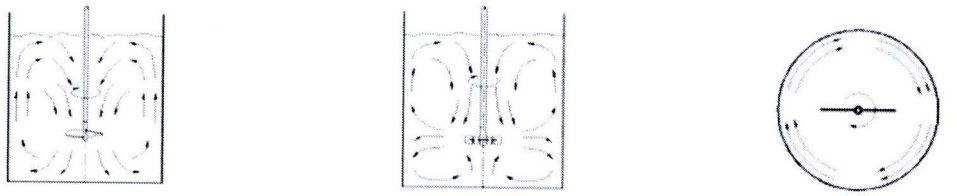

Figure 3.13 Fluid-flow patterns (McCabe, *et al.*, 2001)

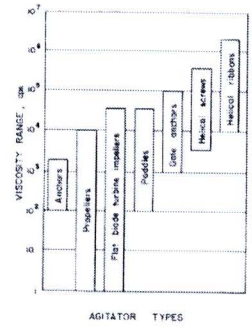

Figure 3.14 The relation between viscosity range and impeller types (Holland, *et al.*, 1966)

3.2.3.1 Axial flow impellers

Axial flow impellers generate currents parallel with the axis of the impeller shape such as marine propeller, hydrofoil and pitched blade turbine as shown in Figure 3.15. They are enhanced the pumping capacity, in addition to be suitable mixed the soluble liquids and between solid and liquid.

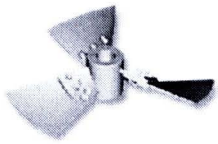

Marine propeller

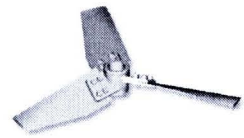

Hydrofoil

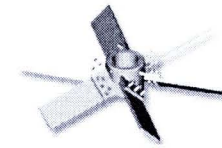

Pitched blade turbine

Figure 3.15 Types of axial-flow impellers (Wellman, 2007a)

3.2.3.2 Radial flow impellers

Radial flow impellers can be categorized in two groups, which are flow in radial direction (six-blade disc turbine and bar disc) and tangential direction (paddle and anchor impeller) as shown in Figure 3.16. For radial direction, the liquids are pushed in outward to the vessel wall and then flow both upward and downward. The impellers can create the high shear zone for mixing immiscible liquids that mean the impellers used for decreasing the particle size of liquids which both liquids can be reacted or mixed easily. For tangential direction, the impeller provides good agitation near the wall and the floor of the tank. It promotes good heat transfer to or form vessel wall and uses to remove the liquids from the tank wall.

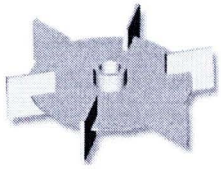

Six-blade disc turbine

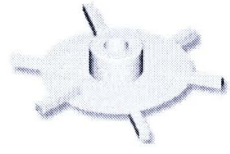

Bar disc

Paddle impeller

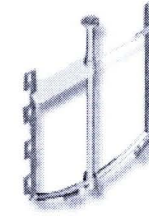

Anchor impeller

Figure 3.16 Types of radial-flow impellers (Wellman, 2007b and Wellman, 2007c)

3.2.4 Dimension of Continuous Stirred Tank Reactors Agitations

Above description, the vertical cylindrical tank having bottom in flat pattern installed four baffles is selected because it is in general agreement. Furthermore, six-blade disc turbine is also selected to install in this reactor because it promotes the mixing of immiscible liquid by creating zone of high shear rate.

The portions of vessel agitations as shown in Table 3.5 can be rearrangement as followed.

The vertical cylindrical tank was chosen as a reactor configuration of this work so the volume of reactor is calculated by using Equation 3.29.

$$V_R = \frac{\pi D_t^2 H_t}{4} \tag{3.29}$$

Table 3.5 indicates that the diameter of reactor is equal to the reactor height. Therefore the new formula of the reactor volume is shown in Equation 3.30 as followed

$$V_R = 0.785 H_t^3 \tag{3.30}$$

Table 3.5 The portions of vessel agitations

Aparatus	Size of CSTR Agitations (cm)	References
Diameter of tank (D_t)	$D_t = H_t$	(McCabe, *et al.*, 2001) (Geonkoplis, 1993)
Height of tank (H_t)	H_t	(McCabe, *et al.*, 2001) (Geonkoplis, 1993)
Baffle width (J)	$J = \frac{H_t}{12}$	(Geonkoplis, 1993)
Diameter of turbine impeller (D_a)	$D_a = \frac{H_t}{2}$	(Geonkoplis, 1993)
Diameter of turbine impeller disc (D_d)	$D_d = \frac{H_t}{3}$	(Geonkoplis, 1993)
Blade width (W)	$W = \frac{H_t}{15}$	(Geonkoplis, 1993)
Blade length (L)	$L = \frac{H_t}{12}$	(Geonkoplis, 1993)
Space between baffle and wall (G)	$G = \frac{0.15H_t}{12}$	(Geonkoplis, 1993)
Diameter of separate tank plate (D_s)	$D_s = H_t$	(Geonkoplis, 1993)
Diameter of hole on separate plate (D_h)	$D_h = \frac{H_t}{3}$	(Geonkoplis, 1993)
Space between turbine and bottom tank (E_s)	$Es = \frac{H_t}{3}$	(McCabe, *et al.*, 2001) (Geonkoplis, 1993)

Due to installation four cylindrical baffles and six-blade disc turbine in the reactor so that the volume of their must be used to calculate for finding the real size of reactor.

The formula for finding four cylindrical baffles volume and six-blade disc turbine are shown in Equation 3.31 and 3.32, which are in term of the reactor height.

The volume of four cylindrical baffles:

$$V_B = \frac{4\pi(H_t/12)^2 H_t}{4} \tag{3.31}$$

$$V_B = 0.022H_t^3 \tag{3.32}$$

The volume of six-blade disc turbine consists of volume of disk, six-blade, axle and axle ring:

$$V_T = V_D + V_{BL} + V_A + V_{AR} \tag{3.33}$$

$$V_T = [6e \times \frac{H_t}{12} \times \frac{H_t}{15}] + [\frac{\pi e}{4} \times \left(\frac{H_t}{3}\right)^2] + [\frac{f^2}{4} \times \pi H_t] + [\frac{\pi}{2} \times \frac{H_t}{15} \times \frac{(f)^2 - (g)^2}{4}] \tag{3.34}$$

$$V_T = 0.120(e)H_t^2 + (0.785f^2 + (0.026(f^2 - g^2)))H_t \tag{3.35}$$

Equation 3.30, 3.32 and 3.35 are combined.

$$V_R = 0.763H_t^3 - 0.120(e)H_t^2 - (0.785f^2 + (0.026(f^2 - g^2)))H_t \tag{3.36}$$

The final equation (Equation 3.36) is obtained in cubic polynomial with the variable of the height of tank, the thickness of turbine, the dimension of axle and the thickness of axle ring. It will be used to estimated the portions of vessel agitations

3.2.5 Conclusions

Equation 3.36 was used to calculation the vessel agitation of CSTR for esterification and of transesterification by setting the thickness of turbine, the dimension of axle and

the thickness of axle ring as 0.2, 0.8 and 0.2, respectively. After obtaining the height of tank value, their standard portions of reactor was substitute with the height of tank value as shown the results in Table 3.6.

Actually, a small calculation cylindrical tube according theory could not be found (esterification). Moreover, a metal rolling machine could not roll the stainless steel plate into the requirement size (transesterification). In order that, the cylindrical tube size of each reactor was increased causing other agitations that were the inside element of reactor were also increased as shown the results in Table 3.6.

Table 3.6 Size of CSTRs agitations for esterification and transesterification

	CSTR agitations for Esterification (cm)		CSTR agitations for Transesterification (cm)	
	Estimation	**Actual work**	**Estimation**	**Actual work**
D_t	8.72	9.70	12.55	14.00
H_t	8.72	9.70	12.55	14.00
Tanks height in series	26.16	29.10	25.10	28.00
Height total	28.78*	32.01*	28.70*	32.20*
J	0.73	0.81	1.05	1.17
D_a	4.36	4.85	6.28	7.00
D_d	2.91	3.23	4.18	4.67
W	0.87	0.97	1.26	1.40
L	1.09	1.21	1.57	1.75
G	0.11	0.12	0.16	0.18
D_s	8.71	9.69	12.54	13.99
D_h	2.91	3.23	4.18	4.67
Es	2.91	3.23	4.18	4.67

*Include 30% of reactor head (Somnuk, 2008)

3.3 Mixing Intensity

3.3.1 Mixing

Initial reagents of biodiesel production such as MCPO, methanol, sulfuric acid, and methoxide solution are the immiscible liquids. Therefore, the mixing of initial reagents is required until it reaches the homogeneous phase. In the first time, the mixing intensity (speed of stirrer) affect on the reaction because the dispersion of initial reagents was not enough. However, when initial reagents is stirred for a moment, ester is occur, which promotes the homogeneous reaction. Consequently, for reducing the mixing time of immiscible liquids, the mixing intensity, which can be

estimated by Reynolds number, will be investigated. In addition, the mixing intensity is necessary to design the reactor and scale it up.

3.3.2 Reynolds Number

From previous work, the FFA reduction and the methyl ester production could be reached in 30 sec. and 5 min., respectively, when Reynolds number around ≥1,680 was used. Therefore, previous Reynolds number was used to estimate the mixing intensity or speed of stirrer by using Equation 3.37 and the other parameters in Table 3.7 and the calculated results in Topic 3.2.4.

$$N_{RE} = \frac{ND_{am}^{2}\rho}{\mu} \tag{3.37}$$

Table 3.7 Initial parameters for estimating the speed of stirrer

	Esterification	**Transesterification**
Total viscosity (Pa.s)	0.02530	0.00896
Total density (kg/m^3)	884.44	864.00
Reynolds number (N_{RE})	1,680	1,680

3.3.3 Mixing Time

Equation 3.38 is used to estimate the retention time for mixing the solution in the reactor. This equation indicates that 5 times of the retention time is required to well mix in the six-blade disc turbine reactor. However, the retention time depended on the size of reactor, of turbine, and the speed of stirrer.

$$t_T = \frac{5}{4} \times \frac{\pi D_{tm}^{2} H_{tm}}{0.92 N_s D_{am}^{2} D_{tm}} \tag{3.38}$$

3.3.4 Conclusions

For the estimation of mixing intensity, it was found that the lower initial speed of stirrer at 1,225 and 213 rpm were used to reduce FFA in 0.836 sec and produce ME in 4.810 sec, respectively. The highly speed of stirrer was used in esterification because

the main reagent (MCPO) had high viscosity more than the main reagent (de-acidified MCPO containing some methanol) in transesterification as shown in Table 4.1. To be according to previous work, although, the speed of stirrer in the actual work should not to less than 1,225 and 213 rpm in esterification and transesterification; it was depended on the motor efficiency.

3.4 Design of Double-Pipe Heat Exchanger in Parallel Flow (Jacket)

3.4.1 Heating Solution in a Parallel Flow Heat Exchanger

Both solutions in esterification and transesterification process will be heated in a parallel flow double-pipe heat exchanger by paraffin oil as shown in Figure 3.15. The length of the heat exchangers (jacket) will be determined. This investigation is assumed that operating conditions and fluid properties (Table 3.8) are constant, and the heat exchanger is well insulated so that heat loss to environment is negligible. In addition, the kinetics and potential energies of fluid streams were also negligible and there was no fouling.

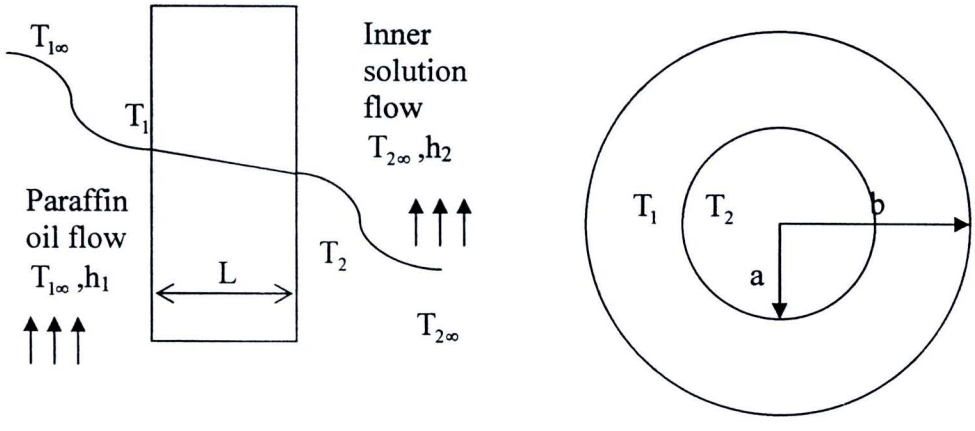

Figure 3.17 Thermal resistance for heat flow through a reactor wall with convection at both surfaces

In Figure 3.17, the heat flow is by convection from hot paraffin oil in jacket to the surface of the outside reactor wall. Then the heat flow is by conduction the reactor wall and by convection from the inside reactor wall to the solution in reactor. The rate

of heat transfer in the heat exchange can be determined by using Equation 3.39 and the temperature of paraffin oil in jacket is determined by Equation 3.40.

$$\dot{Q} = \dot{m} C_p \Delta T \tag{3.39}$$

$$\dot{Q} = A_m h_1 (T_{1\infty} - T_1) = A_m k_m \left(\frac{T_1 - T_2}{L_t} \right) = A_m h_2 (T_2 - T_{2\infty}) \tag{3.40}$$

The convection heat transfer coefficients inside and outside the tube can be determined using the force convection relations. The hydraulic diameter for a circular tube is the diameter of each reactor, which is used to determine the mean of solution in reactor velocity and the Reynolds number as shown in Equation 3.41 and 3.42, respectively.

$$v_m = \frac{\dot{m}}{\rho(\frac{1}{4}\pi D_r^{\,2})} \tag{3.41}$$

$$Re = \frac{v_m D_r}{\nu} \tag{3.42}$$

The Nusselt number can be determined with Equation 3.43 by assuming that the flow to be fully developed. This equation can be investigated from Table 7-1, which is indicted by Çengel (2004).

$$Nu = a_1 \cdot Re^x \cdot Pr^{0.4} \tag{3.43}$$

Then, Equation 3.44 is used to determine the convection heat transfer coefficients inside.

$$h = \frac{k \cdot Nu}{D} \tag{3.44}$$

After that, the hydraulic diameter for the annular space is settle for step by step calculation of the convection heat transfer coefficients outside, which is similar to

determine the convection heat transfer coefficients inside. Finally, both the convection heat transfer coefficients inside and outside are used to determine the temperature of paraffin oil. This investigate will be design the reactor in cylinder shape. Therefore, the logarithmic mean area is used Equation 3.45 and Figure 3.17, which is shown the calculation step in Equation 3.45-3.47.

$$A_m = \frac{A_o - A_i}{\ln(A_o / A_i)} \tag{3.45}$$

$$A_o = 2\pi r_o H_n \tag{3.46}$$

$$A_i = 2\pi r_i H_n \tag{3.47}$$

Table 3.8 Solution properties for solving the size of jacket

Properties	1st solution*	2nd solution*	Paraffin oil	References (paraffin oil)
Density, kg/m^3	884.440	864.000	825.000	(http://www.cartage.org.lb, 2008) and (Wikipedia, 2008a)
Viscosity, $Pa \cdot s$	2.530×10^{-2}	8.960×10^{-3}	1.900	(http://www.cartage.org.lb, 2008)
Kinematics viscosity, m^2/s	2.860×10^{-4}	1.037×10^{-5}	2.315×10^{-3}	-
Specific heat at constant pressure, KJ/kg· °C	1.996	2.050	2.130	(http://www2.ucdsb.on.ca, 2008)
Thermal conductivity, W/m· °C	0.174	0.176	0.250	(The Engineering ToolBox, 2008)
Mass flow rate, kg/s	1.230×10^{-2}	9.960×10^{-2}	0.220	-

*Appendix B and C

After that the flow rate of paraffin oil, the surface area and the length of heat exchanger is determined by Equation 3.39, 3.48 and 3.49, respectively.

$$Q = UA_s\Delta T_p \tag{3.48}$$

$$A_s = \pi D_r L_j \tag{3.49}$$

Özişik (2000) indicated that, the overall heat transfer coefficient base on the outer reactor surface is usually used in the heat exchanger applications. The overall heat transfer coefficient can be expressed as the thermal resistance base on the outside

surface of the reactor. Therefore, the overall heat transfer coefficient can be determined by using Equation 3.51.

$$U_o = \frac{1}{A_o R} \tag{3.50}$$

$$U_o = \frac{1}{(D_o / D_i)(1/h_2) + (1/2k)D_o \ln(D_o / D_i) + 1/h_1} \tag{3.51}$$

If the length of jacket is higher than reactor length, fins should be used for increasing the surface area of reactor, which can reduce the length of jacket. The number of fins can be determined by Equation 3.52.

$$n = \frac{Ws}{S + t} \tag{3.52}$$

3.4.2 Conclusions

The length at 25.00 cm. and the diameter at 25.00 cm. (including the diameter of reactor) were established in estimation of esterification jacket size. The dimension of transesterification jacket at 25.00 cm in length and at 27.60 cm in diameter (including the diameter of reactor) was also obtained. Paraffin oil at 60.12 and 68.89 °C was used for heating solution in esterification and transesterification, respectively.

3.5 Design of Continuous Gravity Decanter Separation

Several methods can be used to separate immiscible liquids such as continuous gravity decanter, centrifugal decanter and hydro-cyclone. This investigation is purposed to separate the two liquids (de-acidified MCPO: the first stage waste, and crude biodiesel: crude glycerin) which are the large different density as shown in Appendix A, so that the continuous gravity decanter separation is considered to separate the immiscible liquids in reasonable time.

3.5.1 Principle of Continuous Gravity Decanter Separation Calculation

Continuous gravity decanter in horizontal cylinder is used to separate the different density two liquids. The slowly flow of feed mixture enters at the one end of the separator and then the mixture separates into two layers. After that, the two liquids discharge through overflow lines at the other end of the vessel.

3.5.1.1 Requirement Time

First of all, the required time for separating the immiscible liquids should be recognized the establishment of the size of decanter. The separation time depends on the difference between the densities of two liquids and on the viscosity of the continuous phase as shown in Equation 3.53.

$$t_s = \frac{100\mu_t}{\rho_A - \rho_B} \tag{3.53}$$

3.5.1.2 Size of Decanter

After that, the length and diameter of decanter is estimated by using the relationship between the separated time, the mixing flow rate and the cross section area of decanter as shown in Equation 3.54. In addition, the length of the decanter should be about 5 times of diameter and the existent volume of the separate tank is 95 % of the full vessel. After establishing the full size of the continuous gravity separated decanter, the height of liquid overflow will be calculation by using Equation 3.55.

$$L_d = \frac{Q \times t_s}{A_d} \tag{3.54}$$

$$Z_{A2} = Z_{A1} + (Z_T - Z_{A1}(\frac{\rho_B}{\rho_A})) \tag{3.55}$$

3.5.2 Conclusion of Continuous Gravity Decanter Separation Design

The principle design of continuous gravity separated decanter, the total viscosity and total densities of two liquids (Table 3.7) were used to calculation the size of decanter and the height of the liquid over flow as shown in Table 3.8.

Table 3.9 Size of continuous gravity decanter separation for esterification and transesterification

	Esterification	**Transesterification**
Separation time (hr.)	3.67	0.91
Length of decanter (cm.)	187.25	121.36
Diameter of decanter (cm.)	38.41	24.92
Decanter value (L)	206.15	56.19
Full decanter value (L)	217.00	59.15
Liquid depth, Z_t (cm.)	34.57	22.42
Heavy phase depth, Z_{A1} (cm.)	17.28	11.21
Light phase depth, Z_B(cm.)	17.28	11.21
Feed hold, Z_{A1}(cm.)	17.28	11.21
Light liquid overflow, Z_t (cm.)	34.57	22.42
Heavy liquid overflow, Z_{A2} (cm.)	31.82	21.07

3.6 Design of Methanol Distillatory

Normally, the production cost of biodiesel is higher than diesel due to the cost of vegetable oil and excess methanol, which are used in the process. To control the production cost of biodiesel, raw material cost (vegetable oil and methanol) have to be reduced. It is found that the price of vegetable oil can not be reduced because it is depended on marketing mechanisms. The simply method to control the price of pure biodiesel is to reduce the utilization of methanol by recovering excess methanol containing in crude biodiesel and waste.

3.6.1 Estimation of Minimum Number of Plates in Methanol Distillatory

McCabe-Thiele Method is generally used to estimate the number of plate in methanol distillatory. In experiment, methanol is recovered from the solution of methanol-water, of methanol-crude biodiesel and of methanol-glycerol. It is found that McCabe-Thiele Method can not used to estimate the plate number in methanol distillatory because it does not have equilibrium curve of methanol-crude biodiesel

and of methanol-glycerol. Therefore, a simple method based on the relative volatility (the ratio of the vapor pressure) of the two components is used to calculate the minimum number of plate from the terminal concentration of mass fraction or mole fraction in bottom and in overhead product, which is defined in term of the equilibrium concentrations.

3.6.1.1 The Minimum of Plates

The equilibrium concentrations of two components is defined by an ideal mixture follows Raoult's law and the relative volatility (McCrabe, 2001), which is the ratio of the vapor pressure as shown in Equation 5.36

$$\alpha_{AB} = \frac{P'_A}{P'_B} \tag{3.56}$$

The minimum number of plate can be solved by using Table 3.10, and Equation 3.56 and 3.57 (McCrabe, 2001). In addition, the mass fractions in bottom and in overhead product are fixed at 0.01 and 0.99, respectively.

$$N_{min} = \frac{\ln[x_D(1-x_B)/x_B(1-x_D)]}{\ln \alpha_{AB}} \tag{3.57}$$

Table 3.10 Vapor pressure of components

Components	Temperature (°C)	Vapor pressure (kPa)	Reference
Glycerol	60.00	8.933×10^{-4}	Jungermann,1991
	70.00	2.266×10^{-3}	
Methyl ester	59.50	5.000×10^{-4}	Genderen, 2002
	61.25	8.000×10^{-4}	
Water	60	19.947	Çengel, et al., 2008
	65	25.043	
Methanol	64.8	101.124	Department of Chemical and Materials Engineering, University of Alberta, 2009

3.6.1.2 Conclusions

In the estimation, the minimum stages for distilling methanol from the solution of methanol-water, of methanol-biodiesel and of methanol-glycerol was shown in Table

3.11. The results indicated that the distillatory tower of methanol-water solution has a large number of plates more than other solution because the water could be evaporated at the boiling point of methanol more than other solution as could be seen the vapor pressure in Table 3.10. However, in simulation process (Chapter 4), it was found that two plates of methanol-biodiesel distillatory and of methanol-glycerol distillatory were the minimum plate number that could be input in the block of distillation. Therefore, the plate number of plate in simulation process was used for fabricating the distillatory in this work.

Table 3.11 The minimum number of plate in methanol distillatory

Solution	Number of stage		
	Design	Design include 40% of equipment efficiency	Simulation
Methanol-water	4.7097	~7	7
Methanol-biodiesel	0.1350	~1	2
Methanol-glycerol	0.0265	~1	2

3.6.2 Design of Sieve-Plate Columns

After estimating the plate number of methanol distillatory, the complete design will be investigated. The investigation (McCabe, 2001) of distillation tower design indicates that tower diameter and plate spacing (plate n to plate n-1) of distillatory should not be less than 30 and 15 centimeter, respectively as shown in Figure 3.18. In addition, each downcomer usually occupies 15 % of the column cross section, and for bubbling or contacting, each downcomer should be living 80 % of the column length. The plate hole should not be less than 0.5 centimeter. Moreover, to permit some degassing of the liquid before it passes over the weir, one or two rows of holes may omit near the overflow weir.

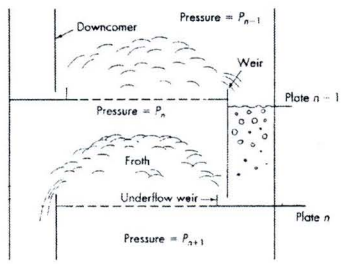

Figure 3.18 Normal operation of sieve plate in methanol distillation tower

(McCrabe, 2001)

3.6.3 Design of Condenser

3.6.3.1 Condenser

Methanol in vapor phase flowing in the jacket is condensed with ambient temperature water flowing in the inner pipe of a double pipe heat exchanger as shown in Figure 3.19.

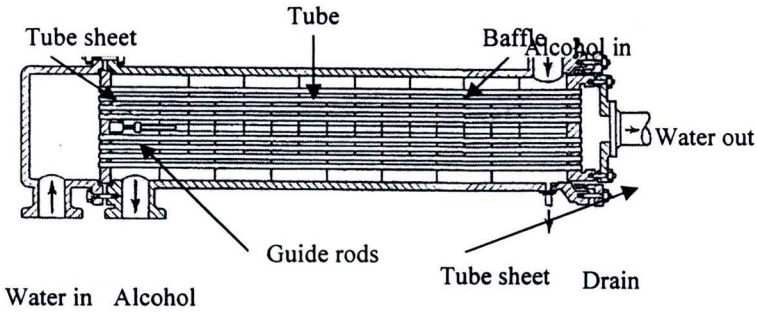

Figure 3.19 Methyl alcohol condenser (McCrabe, 2001)

The rate of heat transfer in the heat exchange can be determined by using Equation 3.41 (Çengel, 2004). After that the surface area and the length of cooler is determined by Equation 3.58 and 3.59, respectively (Çengel, 2004).

$$\dot{Q} = UA_s\Delta T_{lm} \tag{3.58}$$

$$A_s = \pi D_r L_j \tag{3.59}$$

The overall heat transfer coefficient can be determined by using Equation 3.60 (McCabe, 2001).

$$\frac{1}{U} = \frac{1}{\frac{1}{h_i} + \frac{x_w}{k_m} + \frac{1}{h_o}} \tag{3.60}$$

Table 3.12 The properties of water at 25 °C (Çengel, 2004)

Properties	Water
Density, kg/m^3	997.000
Viscosity, Pa.s	0.891×10^{-3}
Kinematics viscosity, m^2/s	8.937×10^{-7}
Specific heat at constant pressure, KJ/kg· K	4.108
Thermal conductivity, W/m·°C	0.697

The convection heat transfer coefficient inside the tube (water) is determined similar to the step of jacket estimation (Topic 3.4) by using the properties of water at Table 3.12. The mean velocity of the solution in inner tube is fixed at least 0.9 m/s and the inner tube is made from 5/8 in. (15.9 mm.) BWG no. 18 tube data indicating by McCabe (2001). Moreover, the convection heat transfer coefficient outside the tube (methanol alcohol) is fixed at 1,000 $W/m\cdot^{\circ}C$ giving from the least of condensing organic vapor in Table 11.2 of McCabe (2001) handbook. The result indicated that length of cooling tube is around 90 centimeters.

3.6.3.2 Condensation of Methanol vapor on Horizontal Tube Banks

After getting the length of tube, it is cut into 9 horizontal tubes of 10 centimeters per tube and arranged the horizontal tube in a square (3×3 tubes). Therefore, the average heat transfer coefficient for vertical tier of 3 horizontal tubes, which is related to the one for a single horizontal tube getting in Topic 3.6.3.1, is determined by Çengel (2004) in the topic of horizontal tube banks as shown in Equation 3.61.

$$h_{\text{horizontal,n tube}} = \frac{1}{N^{\frac{1}{4}}} h_{\text{horizontal,1 tube}} \tag{3.61}$$

Subsequently, the heat transfer coefficient for vertical tier of 3 horizontal tubes is used to recalculate the rate of heat transfer. The result of calculation indicated that 9 horizontal tubes of 10 centimeters per tube, which was arranged in a square (3×3 tubes) has enough rate of heat transfer for cooling the methanol vapor from distillation.

3.6.4 Purification System

After draining glycerol which occurred in transesterification batch process, crude biodiesel was washed four times under ambient temperature. In the first two times, the ambient-temperatured water was sprayed over the surface of the solution until the water volume was equal to the biodiesel volume. After 15 minutes, the washing water was drained. Subsequently, in the third time, the ambient-temperatured water at equal volume to the biodiesel was sprayed over the surface of solution again and then the solution was washed with a bubble technique for 15 minutes. Next, the solution was left for 15 minutes and the washed water was again drained. In the forth and final time, the method was similar to the third time; however, the bubble technique was extended to around 8-12 hours. Finally, after draining, the cleansed solution was heated until it was clear (Suwanmanee, 2006). Not only was heating used to remove the remained moisture in biodiesel, centrifuge and salt adsorption could also be used (Teall, *et al.*, 2003; Zullaikah, *et al.*, 2005). For saving water consumption and reducing time for de-moisture content, dry washing was offered to purify crude biodiesel by ion exchanging with resin, amberlite and purolite, or absorbing with silicates, magnesol (magnesium silicates) and trisyl (Schroeder Biofuels, 1946).

Resin (Lewtit® GF 202: a macroporous cation exchange) was used as adsorbent in dry washing continuous system of this work. Due to resin having high price, Bayer Thai Co., Ltd. (Ion Exchange Resins Group) was assisting this work with giving 0.7 L of resin. Although the obtained resin was not enough to use in full scale of biodiesel production, it was adequate for using in LAB scale. Therefore, the column of biodiesel purification was fabricated according to the guide for laboratory tests with Lewitt Ion Exchanges that Bayer Thai Co., Ltd. (Ion Exchange Resins Group) provided for this work as shown parameters in Table 3.13.

Table 3.13 The portions of resin column

Column	Dimensions
Resin volume (L)	0.6
Diameter (cm)	5
Bed Depth (cm)	30
Column height (cm)	50

3.7 Conclusions

- The design of the two-stage process continuous stirred tank reactor as shown in Figure 3.20 and Appendix D indicated the reactor (the six-blade disc turbine reactor installed with 4 baffles) capacity of 1.5 L (esterification) and 3 L (transesterification) separating into 3 and 2 tank for reducing FFA in MCPO to less than 1 wt% by esterification and producing ME to more than 97 wt% by esterification, respectively. The highest concentration of FFA and TG could be used in the CSTR of this work were 35 wt% and 100 wt%, respectively.

- The size of reactor depended on the reaction rate of each reaction and the flow rate of feeding solution. The six-blade disc turbine reactor installed with 4 baffles was used in this process, which was found that the vessel agitation size was related to the height and the diameter of vessel.

- After establishing the reactor and vessel agitation size, the speed of stirrer, which depended on the viscosity of solution, was determined. The lower initial speed of stirrer at 1,225 and 213 rpm were used to reduce FFA in 0.836 sec and produce ME in 4.810 sec, respectively.

- Double-pipe heat exchanger in parallel flow was estimated for heating the solution in the reactor to reach the required temperature (60 °C). It was found that paraffin oil around 60 - 69 °C was used when the length of jacket was 25.00 and 25.00 cm. and the diameter of jackets was 17.00 and 27.60 cm. (including the diameter of reactor) for esterification and transesterification, respectively.

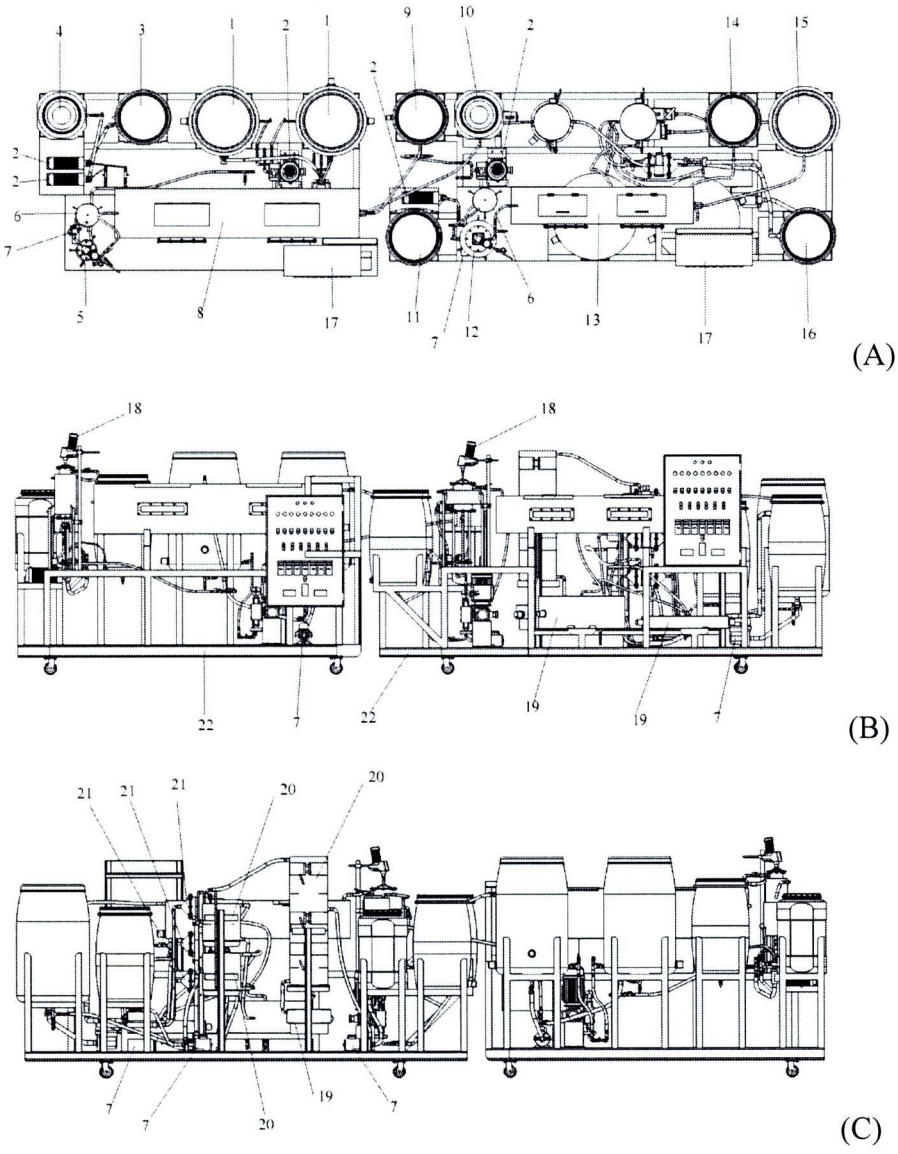

1. MCPO storage tank
2. Metering pump
3. Methanol storage tank
4. Sulfuric acid storage tank
5. CSTR of esterification
6. Hot paraffin oil tank
7. Pump
8. Separate tank of esterification
9. De-acidified MCPO storage tank
10. 1st-stage waste solution storage tank
11. Potassium methoxide solution storage tank
12. CSTR of transesterification
13. Separate tank of transesterification
14. Crude glycerol storage tank
15. Crude biodiesel storage tank
16. Water tank
17. Controller
18. Stirrer motor
19. Re-boiler
22. Distillation tower
25. Condenser
26. Base

Figure 3.20 Top view (A), front view (B) and back view (C) of the two-stage continuous process

- At the end of the process, the solution was separated by horizontal cylinder continuous gravity decanter, which sized 217 L for esterification and 59.15 L for cransesterification. The results indicated that both the densities of two liquids and the

viscosities of the continuous phase were affected on the separated time and separated agitation size.

- The minimum plates for distilling methanol from the solution of methanol-water, of methanol-crude biodiesel and of methanol-glycerol were 7, 2 and 2, respectively. The number of distillation methanol plates was depended on the vapor pressure of each compound in solution.

- The condenser for cooling the vapor phase of methanol was consisted of 9 horizontal tubes sizing of 10 centimeters per tube and it was arranged into horizontal tube in a square (3×3 tubes).

- Due to high price of resin, the purification of biodiesel in LAB scale was investigated. Therefore, drawing of it was not shown in the Figure 3.20 and Appendix D. The total volume of column was 981.75 cm^3 that contained resin of 0.6 L in bed depth at 30 cm.